Journal of Power Sources 184 (2008) 303–307

Contents lists available at ScienceDirect

Journal of Power Sources

journal homepage: www.elsevier.com/locate/jpowsour

Short communication

Effects of reactant dispersion on the structure and electrochemical performance of $Li_{1.2}V_3O_8$

Yongmei Liu, Xuechou Zhou, Yonglang Guo*

College of Chemistry and Chemical Engineering, Fuzhou University, Fuzhou 350108, PR China

ARTICLE INFO

Article history:
Received 17 November 2007
Received in revised form 30 May 2008
Accepted 11 June 2008
Available online 21 June 2008

Keywords:
Lithium trivanadate
Lithium-ion battery
Low-temperature
Ultrasonic treatment
Structure and morphology

ABSTRACT

The pure-phase $Li_{1.2}V_3O_8$ was synthesized by ultrasonically dispersing Li_2CO_3 and NH_4VO_3 reactants. Its structure and morphology compared with the pristine $Li_{1+x}V_3O_8$ obtained from the solid-state reaction were investigated by X-ray diffraction (XRD) and scanning electron microscope (SEM). The results show that the compound synthesized at 570 °C from the precursor obtained by ultrasonic treatment in anhydrous ethanol has low crystallinity and homogeneous morphology with bar-like shape. Charge–discharge cycling, cyclic voltammetry (CV) and electrochemical impedance spectroscopy (EIS) experiments indicate that this sample has relatively high initial discharge capacity and good cycle ability, and it is beneficial to the reversible insertion/extraction of Li^+ ions because of the low kinetic resistance. Its discharge capacity reaches 270 mAh g^{-1} in the 2nd cycle at 0.2 C discharge rate and still retains 210 mAh g^{-1} in the 100th cycle in the range of 2.0–4.0 V.

1. Introduction

Recently, the production of lithium-ion batteries continues to expand with the increasing demand from the electronics devices, e.g. cellular phones and various portable electrical products. The commercial lithium-ion batteries mainly use cobalt-based oxides as the positive electrode. Due to its high cost and some toxicity, lithium cobalt oxide ($LiCoO_2$) is gradually replaced by other transitional metal oxide. Layered $Li_{1+x}V_3O_8$ is a promising candidate for positive materials because of its high capacity, low cost, long cycle life, facile preparation and stability in air [1–4]. However, the preparation methods have significant effects on its electrochemical properties. Traditional synthesis of $Li_{1+x}V_3O_8$ is the solid-state reaction of Li_2CO_3 and V_2O_5 at 680 °C [5]. At such high reaction temperature, it is difficult to control the accurate ratio of lithium to vanadium atom because of the reactants evaporation. Meanwhile, the specific capacity is low (180 mAh g^{-1}) and molten V_2O_5 would cause the corrosion of the crucible.

In order to improve its electrochemical behavior such as discharge capacity and cycle performance, many researchers have focused on the post-treatments and synthesis routes of $Li_{1+x}V_3O_8$. Post-treatments include the ultrasonic treatment in water solution [6], efficient grinding [7], and intercalation of small inorganic molecules between layers [1], which can improve the performance of $Li_{1+x}V_3O_8$, but often require complicated steps and extra equipments. So the methods above are not suitable for large-scale production. The different heating temperatures in the $Li_{1+x}V_3O_8$ synthesis have great effects on its crystallinity and electrochemical performance. In general, the materials synthesized at lower temperature have lower crystallinity, higher initial capacity and rapid capacity deterioration, compared with those synthesized at melting point. These low-temperature syntheses have this in common, that is to disperse the reactants containing lithium and vanadium atoms into the solvent (H_2O or CH_3OH) to obtain precursors, and then heat the precursors at different temperatures [2,4,8–13]. For example, Liu et al. [2] synthesized $Li_{1+x}V_3O_8$ from the precursor obtained with LiOH and V_2O_5 in aqueous solution. The material exhibited severe capacity deterioration. Kannan et al. [13] heated the precursor of LiV_3O_8 at 500 °C in N_2 atmosphere, which was obtained by stirring the dispersion of reactants (LiOH and NH_4VO_3) in methanol. The material had around 230 mAh g^{-1} initial capacity at 0.5 mA cm^{-2} in the voltage range of 2.0–3.5 V with preferable cycle ability. However, water should be excluded from the non-aqueous lithium cell and methanol (CH_3OH) is toxic. In addition, ultrasonic dispersion has been used to synthesize other cathode materials of lithium-ion batteries, which has the uniform particle distribution and higher electrochemical performance [14–16]. In the present work, $Li_{1.2}V_3O_8$ was synthesized at low temperature from the precursor with ultrasonic treatment and then its structure and electrochemical performance were investigated.

* Corresponding author. Fax: +86 591 8789 2893.
E-mail address: yguo@fzu.edu.cn (Y. Guo).

0378-7753/$ – see front matter © 2008 Elsevier B.V. All rights reserved.
doi:10.1016/j.jpowsour.2008.06.031

2. Experimental

2.1. Synthesis and characterization of samples

Stoichiometrically weighted Li_2CO_3 and NH_4VO_3 (molar ratio: Li:V = 1.2:3) were blended in 40 ml anhydrous ethanol (CH_3CH_2OH) and stirred for several minutes. The suspended materials were treated by a KH-50B ultrasonic instrument for 90 min, followed by spontaneous evaporating ethanol at room temperature, then the mixtures were heated at 120 °C for 4 h in vacuum to remove residual ethanol and get the precursor. Finally, the product was obtained by calcining the precursor at 570 °C (lower its melting point of $Li_{1+x}V_3O_8$ (601 °C)) for 8 h at dry air atmosphere (sample a). In comparison, the synthesis conditions of sample b are the same as sample a, but without the ultrasonic treatment. Samples c and d were prepared by the conventional solid-state reaction method from the well-milled stoichiometric mixtures of Li_2CO_3 and NH_4VO_3 at 570 and 680 °C in air for 8 h, respectively and then they were ground after cooling to room temperature. The precursor with the ultrasonic treatment and its corresponding product were analyzed by thermogravimetry (TG) and differential scanning calorimetry (DSC) to determine the reaction processes. The TG–DSC tests were performed on SDTQ600 thermoanalyzer at a heating rate of 10 °C min^{-1} in air. The X-ray diffraction (XRD) was carried out using the X'pert Pro MPP X-ray diffractometer with Cu Kα radiation (λ = 1.54056 Å) to identify the structure of the synthesized materials. Their morphologies were observed by a scanning electron microscope (SEM, Philips, XL30 ESEM-TEP).

2.2. Electrochemical measurements

The electrochemical performance of the synthesized materials was evaluated in model CR2025 coin cells. The paste consisted of the active material prepared above, acetylene black and polyvinylidene fluoride (PVDF) in the weight ratio of 85:10:5. The positive electrode was prepared by coating the paste on Al collector. Lithium foil served as the negative electrode. The separator was Celgard 2320 membrane and the electrolyte was 1 M $LiPF_6$ in ethylene carbonate (EC) and dimethyl carbonate (DMC) in volume ratio of 1:1. Cyclic test of these cells at different charge–discharge rates between 2.0 and 4.0 V was performed by Land automatic battery tester (Wuhan, China). Cyclic voltammetry (CV) and the electrochemical impedance spectroscopy (EIS) were performed on the positive electrode in the cells described above by a CHI 660C electrochemical work station. The EIS measurements were carried out by applying an ac voltage of 2 mV in the frequency range of 10 mHz–100 kHz on open circuit voltage after charging to 3.5 V. All cells were assembled in a glove box filled with pure argon gas and tested at room temperature.

3. Results and discussion

3.1. The TG–DSC analysis

Fig. 1 shows the TG–DSC curves of the precursor obtained by ultrasonic treatment in anhydrous ethanol and its calcined product, respectively. It is found from Fig. 1A that the weight loss is about 26.5% in the range of 150–570 °C and remains unchanged above 570 °C. The weight loss process can be divided into two main steps. The first weight loss is about 16% in the range of 100–285 °C and two DSC peaks appear at 197 and 234 °C, which resulted from the evaporation of NH_3 and the deintercalation of water from $NH_4V_3O_8$ [4]. The second weight loss is about 10.5% in the range of 285–570 °C, the DSC endothermic peak at 305 °C was caused by the removal

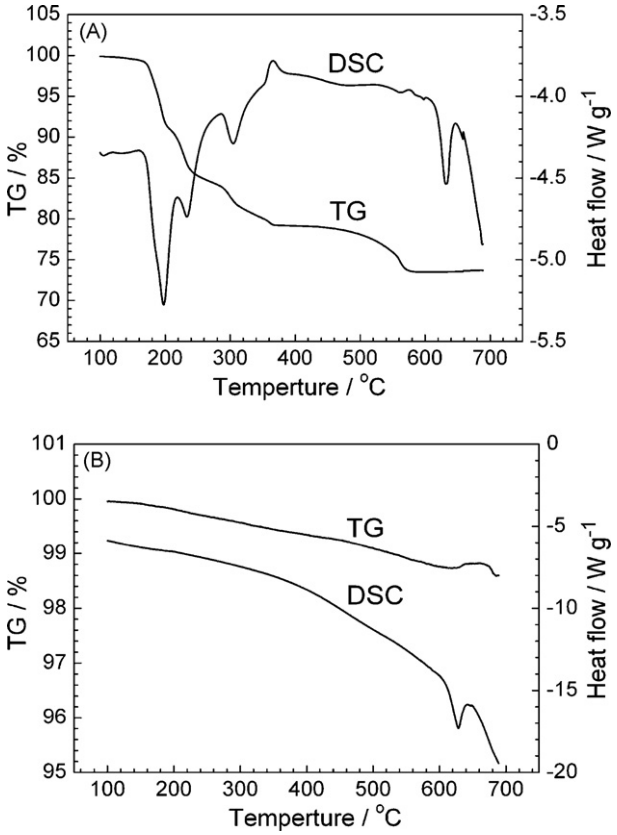

Fig. 1. TG–DSC curves of (A) $Li_{1.2}V_3O_8$ precursor with ultrasonic treatment and (B) its corresponding product. Heating rate: 10 °C min^{-1}.

of water in $Li_{1.2}V_3O_8{\cdot}nH_2O$ [9] and the mild exothermic peak at 360 °C may be explained by the structural densification induced by squeezing the remained water out of the structure of $Li_{1.2}V_3O_8$ [11]. The obvious endothermic peak at 630 °C without weight loss is due to the melting of $Li_{1+x}V_3O_8$. The total weight loss (26.5 %) in 150–570 °C agrees well with the calculated value (26.8%). Since no obvious weight loss occurs in the range of 150–700 °C in Fig. 1B, the synthesis reaction is considered to be completed. To reduce the evaporation of the reactants, therefore, 570 °C is chosen as the calcination temperature in this work, which is lower than the melting point of $Li_{1+x}V_3O_8$.

3.2. Sample characterization

Chemical analyses and redox titration were used to analyze the composition of samples. The results indicated that the compositions of samples a, b and c are $Li_{1.2}V(VI)_{0.2}V(V)_{2.8}O_8$, yet a little V(III) in sample d is difficult to be analyzed. So sample d is expressed as $Li_{1+x}V_3O_8$. Fig. 2 shows the XRD patterns of the materials calcined at 570 °C under different reactant dispersion conditions and at 680 °C by solid-state reaction. All diffraction lines can be indexed in JCPDS card (No. 72-1193) with space group $P21/m$ without any impurity phases. And the X-ray patterns of the materials prepared at 570 °C fairly well match the pattern obtained at the high temperature (680 °C). However, the great difference lies in the distribution of peak intensity. The material synthesized at high temperature (sample d) has the sharpest peak for the (1 0 0) plane, indicating that it has the largest dimension along (1 0 0) planes corresponding to layers of VO_n polyhedra. Thus the diffusion paths of the lithium ion insertion between these planes become longer [17], which is disadvantageous to its electrochemical properties. It can also be

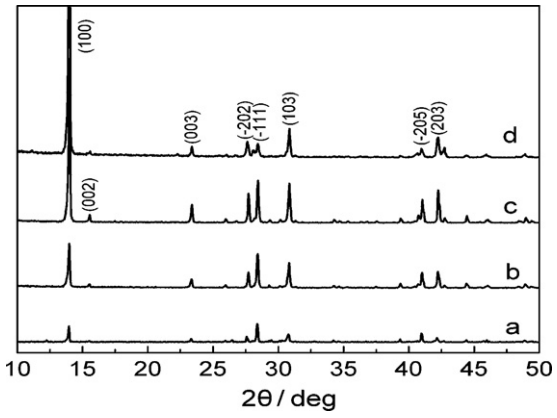

Fig. 2. The XRD patterns of $Li_{1.2}V_3O_8$ synthesized at 570 °C from precursors (a) with and (b) without ultrasonic treatment; and $Li_{1+x}V_3O_8$ by solid-state reaction at (c) 570 °C and (d) 680 °C.

seen from Fig. 2 that the lower intensity of (1 0 0) peaks for the samples synthesized at 570 °C (i.e. sample a, b and c) is related to the reactant dispersal conditions. The dispersing reactant in liquid phase reduces their diffraction peaks greatly. The peaks intensity of sample a, which was synthesized by ultrasonic treatment, is the weakest, indicating that sample a has the lowest crystallinity and, in a way, some isotropic property.

Fig. 3 shows the SEM images of the samples calcined at 570 °C from precursors with and without the ultrasonic treatment in anhydrous ethanol, respectively. It is seen that the different treatments

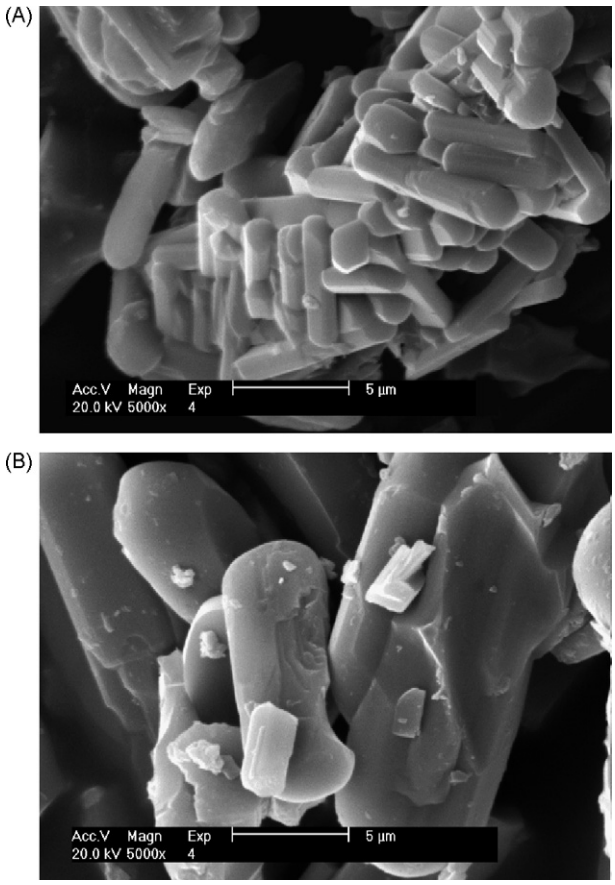

Fig. 3. SEM of $Li_{1.2}V_3O_8$ synthesized at 570 °C from precursors (A) with (sample a) and (B) without ultrasonic treatment (sample b).

of the precursors can obviously affect the morphology of products. Sample a synthesized from the precursor with the ultrasonic treatment is made up of homogeneous short bar-like grains with uniform distribution (Fig. 3A), while sample b synthesized from the precursor without the ultrasonic treatment has lumpish particles with larger size (Fig. 3B). Based on the XRD and SEM results, it is obvious that the synthesis from the precursor dispersed by the ultrasonic treatment described above can get the uniform product with smaller particles and larger specific surface area and to some extent isotropic property. The effects of reactant dispersion with ultrasonic treatment on the structures and morphologies of the products can be explained as follows. In solid–liquid mixtures, the solid powders are uniformly dispersed in liquid phase. So in comparison with the solid-state synthesis, their surface area is more efficiently utilized due to the close contact between the solid reactants, which can promote the formation of the $Li_{1.2}V_3O_8$ nuclei and small particles. It is also convenient for the heat exchange and the diffusion of lithium into the material [18]. The assistant ultrasonic process could make the solid powders dispersed more uniformly in the liquid substances and restrain the agglomeration of solid powders, thus the product with the small particles and uniform distribution can ultimately be obtained.

3.3. Electrochemical properties

Fig. 4 shows the cyclic performance of the samples at 0.2 C discharge and charge rates in the range of 2.0–4.0 V. It can be seen that sample a synthesized from the precursor with the ultrasonic treatment gives the highest initial discharge capacity and the best cyclic performance. Its reversible capacity is about 270 mAh g^{-1} in 10 cycles. Although sample b has also a high initial discharge capacity (254 mAh g^{-1}), its capacity drops rapidly to 214 mAh g^{-1} in the third cycle and remains stable in the following seven cycles. In comparison, the capacity of samples c and d is also examined. Their specific capacity is lower than that of samples a and b. These phenomena are in agreement with the XRD and SEM results, which are related with the structure and morphology of the synthesized materials. Samples a and b have relatively large specific surface area, thus they may have more lithium insertion/extraction sites. The isotropic structure property and the homogeneous grains of sample a help keep the structure stable during the cycling, thus showing good cyclic performance. Therefore, the ultrasonic dispersion method can be used to prepare the $Li_{1+x}V_3O_8$ material with high electrochemical performance.

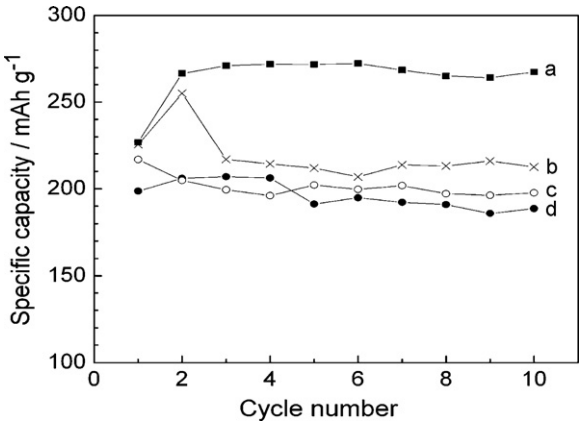

Fig. 4. Cycle performance at 0.2 C rates on $Li_{1.2}V_3O_8$ positive materials synthesized at 570 °C from precursors (a) with and (b) without ultrasonic treatment and $Li_{1+x}V_3O_8$ synthesized by solid-state reaction at (c) 570 °C and (d) 680 °C.

Fig. 5A shows the charge–discharge curves of samples a and d in the 10th cycle. Fig. 5B is their differential capacity (dQ/dV) obtained from Fig. 5A. The $Li_{1+x}V_3O_8$/Li cells were charged and discharged at 0.2 C rate between 2.0 and 4.0 V. It can be seen from Fig. 5A that sample a synthesized from the precursor with the ultrasonic treatment has the discharge capacity of 270 mAh g^{-1} in the 10th cycle and sample d synthesized from the traditional solid-state reaction at 680 °C has only the discharge capacity of 188 mAh g^{-1}. The shapes of the charge–discharge curves of both samples are similar and so are dQ/dV profiles. Generally, there are five pairs of peaks in the dQ/dV plots, which correspond to the plateaus on the charge/discharge curves in Fig. 5A. The sharp peaks in Fig. 5B indicate that the lithium insertion/extraction proceeds through a few multiphase regions until reversible lithium uptake is reached [19]. The anodic/cathodic peaks of sample a is much higher than those of sample d, indicating the higher charge–discharge capacity of sample a.

To further understand the electrochemical behavior of the samples prepared under different conditions, Fig. 6 shows the CV curves of samples a and d in the 2nd cycle at a scan rate of 0.1 mV s^{-1}. It is seen that sample d exhibits an obvious oxidation peak at 2.85 V with corresponding three reduction peaks at 2.76, 2.7 and 2.48 V, respectively, and a pair of unconspicuous redox peaks at around 3.65 V. According to Ref. [20], these redox peaks are related to the x value in $Li_{1+x}V_3O_8$. As for sample a, all oxidation and reduction peaks are sharper and larger in areas than those of sample d and furthermore it has an additional smaller reduction peak at 2.62 V. It suggests that sample a has more sites and faster kinetics for Li^+ insertion/extraction, which is mainly related to the crystallinity and morphology of samples. The splitting cathodic peaks between 2.5 and 2.85 V correspond to lithium insertion in sites with energy difference for holding of Li^+ ions [21].

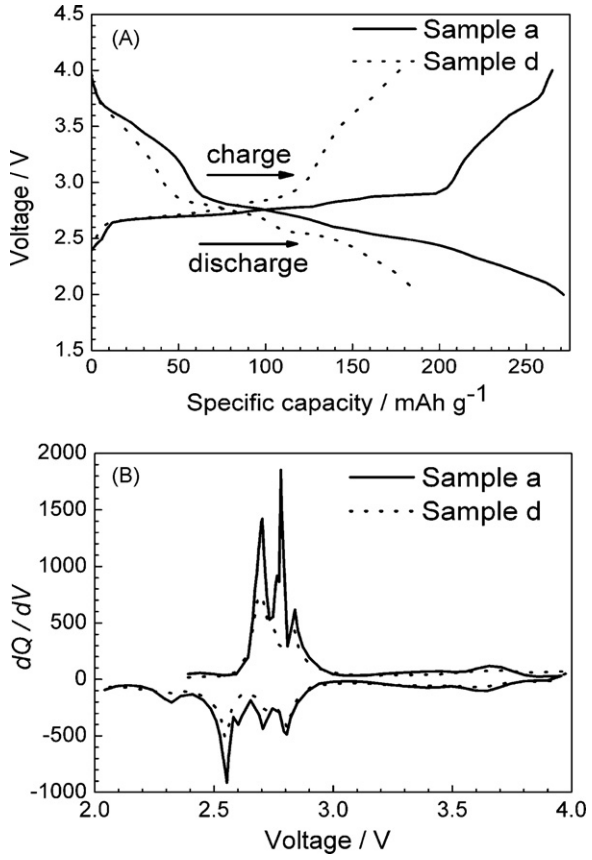

Fig. 5. (A) Charge and discharge curves and (B) dQ/dV vs. voltage plots of $Li_{1.2}V_3O_8$ synthesized at 570 °C from the precursor with ultrasonic treatment (sample a) and $Li_{1+x}V_3O_8$ at 680 °C by solid-state reaction (sample d) (charge and discharge rates: 0.2 C).

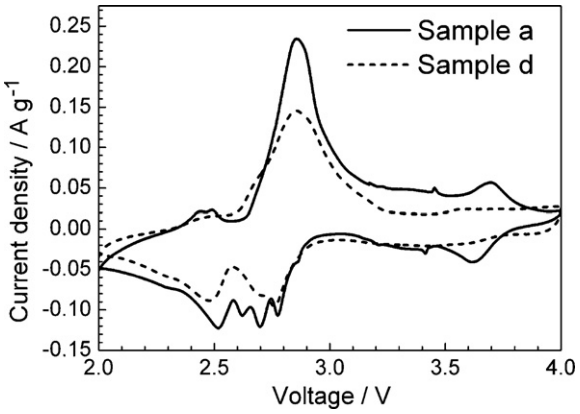

Fig. 6. Cyclic voltammograms of $Li_{1.2}V_3O_8$ synthesized at 570 °C from the precursor with ultrasonic treatment (sample a) and $Li_{1+x}V_3O_8$ at 680 °C by solid-state reaction (sample d). Scan rate: 0.1 mV s^{-1}.

Fig. 7 shows the EIS of the positive electrodes for samples a and c. The tests were carried out on open circuit after the cut voltage of 3.5 V after 2 cycles. The EIS shapes of both electrodes are similar, which are composed of a semicircle and a linear part in the frequency range from 100 kHz to 10 mHz. The semicircle in the high frequencies is attributed to the electron transfer process and the linear part in low frequencies is due to Li^+ ions solid-state diffusion within the electrode [22]. According to the results reported by Chen et al. [23], lithium-ion cell impedance is mainly attributed to cathode impedance, especially charge transfer resistance. The diameter of semicircle on sample a prepared from the precursor with the ultrasonic treatment is obviously smaller than that of sample c synthesized from the solid-state reaction at 570 °C, which implies that the insertion/extraction of Li^+ ions in the $Li_{1+x}V_3O_8$ compound prepared by this new method is easier. This is consistent with the results of XRD and SEM, and that is to say the sample prepared from the precursor with the ultrasonic treatment has better structure and morphology, which are advantageous to its electrochemical performance.

Fig. 8 shows the cyclic performance and the effects of charge–discharge rates for sample a calcined at 570 °C from the precursor with ultrasonic treatment. Curve a is obtained at 0.5 C charge and 0.2 C discharge rates and curve b at 0.1 C charge and 0.2 C discharge rates from 1 to 89 cycles and at 0.1 C charge–discharge rate

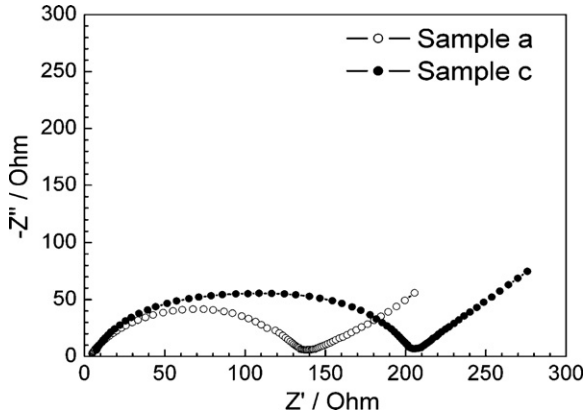

Fig. 7. The EIS of positive electrodes synthesized at 570 °C from the precursor with ultrasonic treatment (sample a) and at 570 °C by solid-state reaction (sample c).

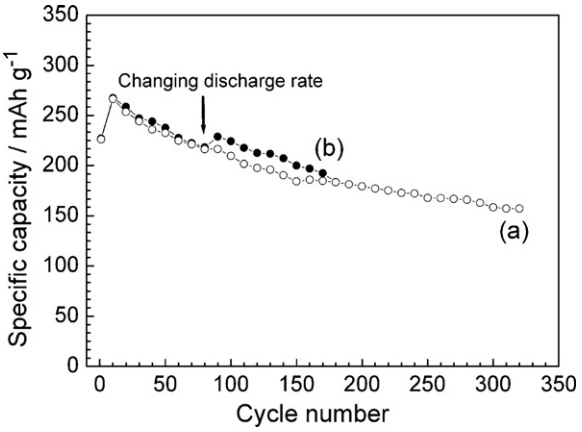

Fig. 8. Specific capacity vs. cycle number of $Li_{1.2}V_3O_8$ synthesized at 570 °C from the precursor with ultrasonic treatment (a) at 0.5 C charge rate and 0.2 C discharge rate; (b) at 0.1 C charge rate and 0.2 C discharge rate from 1 to 89 cycles and 0.1 C charge–discharge rate from 90 to 180 cycles.

from 90 to 180 cycles. It is observed that there is almost no change in the specific discharge capacity on the two curves from 1 to 89 cycles, which indicates that the charge currents have hardly any effect on the discharge capacity when the charge rate changes from 0.1 to 0.5 C. So Li^+ ions can extract very easily from this material in the charge. However, the specific discharge capacity increases obviously on curve b when the discharge rate decreases from 0.2 to 0.1 C in the 90th cycle. It means that the Li^+ ion insertion in the discharge is more difficult than its extraction in the charge. Generally speaking, this sample has relatively good rate capability and cycling performance. At 0.5 C charge and 0.2 C discharge rates, its discharge capacity in the 2nd cycle reaches 270 mAh g^{-1} and can remain 220 and 160 mAh g^{-1} in the 100th and 320th cycles, respectively. Therefore, it is an attractive cathode material for practical application.

4. Conclusions

In this study, a simple and cost-saving method was employed to synthesize $Li_{1.2}V_3O_8$ compound by calcining the Li_2CO_3 and NH_4VO_3 mixtures with ultrasonic treatment in anhydrous ethanol at 570 °C. With the assistance of ultrasonic dispersion, the reactant powders can be uniformly dispersed in the liquid substances, thus improving the heat exchange and the formation of the nuclei in the synthesis. XRD and SEM experiments indicate that the product has isotropic property and homogeneous morphology. The CV and EIS studies indicate that the structure of this compound has more Li^+ ion insertion/extraction sites and it is beneficial to the reversible movement of Li^+ ions. The charge–discharge tests show that this compound exhibits a relatively high initial capacity and good cycling stability. At 0.2 C discharge rates, the discharge capacity is 270 mAh g^{-1} in the 2nd cycle, and it remains 220 mAh g^{-1} in the 100th cycle and about 160 mAh g^{-1} after 320 cycles. All this reveals that this synthesis routine is a promising method for preparing the $Li_{1+x}V_3O_8$ cathode material.

References

[1] V. Manev, A. Momchilov, A. Nassalevska, G. Pistoia, M. Pasquali, J. Power Sources 54 (1995) 501.
[2] Q.Y. Liu, H.W. Liu, X.W. Zhou, C.J. Cong, K.L. Zhang, Solid State Ionics 176 (2005) 1549.
[3] V.L. Piccotto, K. Adendorff, D. Liles, M. Thackeray, Solid State Ionics 62 (1993) 297.
[4] H.Y. Xu, H. Wang, Z.Q. Song, Y.W. Wang, H. Yan, M. Yoshimura, Electrochim. Acta 49 (2004) 349.
[5] S. Panero, M. Pasquali, G. Pistoia, J. Electrochem. Soc. 130 (1983) 1226.
[6] N. Kumagai, A.S. Yu, J. Electrochem. Soc. 144 (1997) 830.
[7] G. Pistoia, M. Pasquali, Y. Geronov, V. Manev, R.V. Moshtev, J. Power Sources 27 (1989) 35.
[8] K. Nassau, D.W. Murphy, J. Non-cryst. Solids 44 (1981) 297.
[9] J.X. Dai, F.Y. Li, Z.Q. Gao, K.S. Siow, J. Electrochem. Soc. 145 (1998) 3057.
[10] G.Q. Liu, C.L. Zeng, K. Yang, Electrochim. Acta 47 (2002) 3239.
[11] J.G. Xie, J.X. Li, H. Zhan, Y.H. Zhou, Mater. Lett. 57 (2003) 2682.
[12] J. Kawakita, Y. Katayama, T. Miura, T. Kishi, Solid State Ionics 110 (1998) 199.
[13] A.M. Kannan, A. Manthiram, J. Power Sources 159 (2006) 1405.
[14] P. Shen, Y. Huang, L. Liu, D. Jia, Z. Guo, J. Solid State Electrochem. 10 (2006) 929.
[15] W.J. Zhou, S.J. Bao, B.L. He, Y.Y. Liang, H.L. Li, Electrochim. Acta 51 (2006) 4701.
[16] T.F. Yi, X.G. Hu, J. Power Sources 167 (2007) 185.
[17] K. West, B. Zachau-Christiansen, S. Skaarup, Y. Saidi, J. Barker, I.I. Olsen, R. Pynenburg, R. Koksbang, J. Electrochem. Soc. 143 (1996) 820.
[18] J. Xiao, H. Zhan, Y.H. Zhou, Mater. Lett. 58 (2004) 1620.
[19] C.Q. Feng, S.Y. Chew, Z.P. Guo, J.Z. Wang, H.K. Liu, J. Power Sources 174 (2007) 1095.
[20] G. Pistoia, M. Pasquali, G. Wang, L. Li, J. Electrochem. Soc. 137 (1990) 2365.
[21] J. Kawakita, M. Majima, T. Miura, T. Kishi, J. Power Sources 66 (1997) 135.
[22] X.M. Wu, X.H. Li, Z. Wang, Z.B. Xiao, J.B. Liu, W.B. Yan, Mater. Chem. Phys. 83 (2004) 78.
[23] C.H. Chen, J. Liu, K. Amine, J. Power Sources 96 (2001) 321.